Very Efficient Visible Light Energy Harvesting and Conversion by Spectral Sensitization of High Surface Area Polycrystalline Titanium Dioxide Films

Nick Vlachopoulos,† Paul Liska,† Jan Augustynski,‡ and Michael Grätzel*†

Contribution from the Institut de Chimie Physique, Ecole Polytechnique Fédérale, CH-1015 Lausanne, Switzerland, and Institut de Chimie Minérale, Analytique et Appliquée, Université de Genève, CH-1211-Genève, Switzerland. *Received August 18, 1987*

Abstract: By using high surface area (roughness factor ca. 200) polycrystalline anatase films together with tris(2,2'-bipyridyl-4,4'-dicarboxylate)ruthenium(II), RuL_3^{4-}, as a sensitizer, we have achieved unprecedentedly high visible light to electric current conversion efficiencies in regenerative photoelectrochemical cells. Incident photon to current conversion efficiencies of 73% have been obtained at the wavelength of maximum absorption of the dye in the presence of iodide as an electron donor. Bromide is oxidized under the same conditions with an efficiency of 56%. A regenerative cell based on the Br_2/Br^- redox system gives a monochromatic light to power conversion efficiency of 12% with a fill factor of 74%. Preliminary results with polychromatic illumination are also presented.

The sensitization of wide band gap semiconductors is a fascinating domain of research which is presently under active investigation.[1] The phenomenon of charge injection from an excited sensitizer in the valence or conduction band is used to effect photoinduced charge separation with light of less than band gap energy.[2] A major problem with the application of spectral sensitization in photoelectrochemical devices for solar energy conversion systems has been low efficiency. Thus, if the dye is merely dissolved in the electrolyte, the excited state lifetime is too short to allow for diffusion to the semiconductor electrode and charge transfer. As a rule, surface attached species alone can contribute to the sub-band gap photoresponse of the device. On such a modified semiconductor surface, only the first adsorbed monolayer can transfer charge, thick dye layers tending to be insulating.[3] However, on a flat surface the absorption by monolayers is at most a few percent, so that the sensitization effect is feeble. Matsumara et al.[4] and Alonso et al.[5] have used sintered ZnO electrodes to increase the efficiency of sensitization by rose bengal and related dyes. We have recently introduced[6] polycrystalline TiO_2 (anatase) films with a surface roughness factor of several hundred that are used in conjunction with dyes which are chemically modified to enhance their adsorption. Incident photon to current conversion efficiencies up to 44% have been obtained so far with these systems which is unprecedented in the domain of spectral sensitization.[7,8] Though similar to a conventional *n*-type photoanode, the dye-sensitized semiconductor operates by electron injection and is therefore a majority carrier device. The high recombination losses due to disorder in a semiconductor structure where the electroactive minority carriers are holes are not encountered in such a case. The present report deals with light-induced halide oxidation on RuL_3^{4-}-(L = 2,2'-bipyridyl-4,4'-dicarboxylate[9])sensitized TiO_2 electrodes. Incident photon to current conversion efficiencies of 73% and 56% have been obtained in the oxidation of iodide and bromide, respectively. A monochromatic light to power conversion efficiency of 12% and a fill factor of 74% has been achieved with the Br_2/Br^- redox system in a regenerative photoelectrochemical cell.

Experimental Section

Preparation of High Surface Area TiO_2 Films. TiO_2 (anatase) films were prepared by thermal decomposition of titanium alcoholate solutions, deposited on the cross section of Ti rods (Kobe Steel, Japan, 99.5% purity, Fe content 0.25%, 6 mm in diameter, and 6 cm in length) or the surface of Ti sheets (Siber Hegner Rohstoff AG, Zurich, Switzerland, ASTM grade 2, size 2 × 2 cm, thickness 0.05 cm). The titanium surface on which the oxide layer was deposited was subjected to a pretreatment consisting of boiling for 0.5 h in 18% HCl. The titanium ethoxide solution was prepared by dissolving 21 mmol of freshly distilled $TiCl_4$ in 10 mL of absolute ethanol (Fluka puriss.). The solution was then diluted

† Institut de Chimie Physique, Ecole Polytechnique Fédérale.
‡ Institut de Chimie Minérale, Analytique et Appliquée, Université de Genève.

(1) (a) Meier, H. *J. Phys. Chem.* **1965**, *69*, 705. (b) Nemba, S.; Hishiki, Y. *J. Phys. Chem.* **1965**, *69*, 724. (c) Gerischer, H. In *Physical Chemistry: An Advanced Treatise*; Academic Press: New York, 1970; Vol. IXA. (d) Tributsch, H.; Calvin, M. *Photochem. Photobiol.* **1971**, *14*, 95. (e) Memming, R.; Tributsch, H. *J. Phys. Chem.* **1971**, *75*, 562. (f) Fujishima, A.; Watanabe, T.; Tatsuji, O.; Honda, K. *Chem. Lett.* **1975**, 13. (g) Gerischer, H. *Photochem. Photobiol.* **1975**, *16*, 243. (h) Gleria, M.; Memming, R. *Z. Phys. Chem. (Munich)* **1975**, *98*, 303. (i) Hauffe, K. *Photogr. Sci. Eng.* **1976**, *20*, 124. (j) Tributsch, H. *Z. Naturforsch., A: Phys., Phys. Chem., Kosmophys.* **1977**, *32A*, 972. (k) Gosh, P. K.; Spiro, T. G. *J. Am. Chem. Soc.* **1980**, *102*, 5543. (l) Memming, R. *Surf. Sci.* **1980**, *101*, 551. (m) Kamat, P. V.; Fox, M. A. *Chem. Phys. Lett.* **1983**, *102*, 379. (n) Krishnan, M.; Zhang, X.; Bard, A. J. *J. Am. Chem. Soc.* **1984**, *106*, 7371. (o) Moser, J.; Grätzel, M. *J. Am. Chem. Soc.* **1984**, *106*, 6557. (p) Rossetti, R.; Brus, L. E. *J. Am. Chem. Soc.* **1984**, *106*, 4336. (q) Shimidzu, T.; Iyoda, T.; Koide, Y. *J. Am. Chem. Soc.* **1985**, *107*, 35. (r) Kamat, P. V.; Chauvet, J. P.; Fessenden, R. W. *J. Phys. Chem.* **1986**, *90*, 1398.

(2) (a) Bourdon, J. *J. Phys. Chem.* **1965**, *69*, 705. (b) Hauffe, K.; Range, J. *Z. Naturforsch., B: Anorg. Chem., Org. Chem., Biochem., Biophys., Biol.* **1968**, *23B*, 736. (c) Gerischer, H.; Michel-Beyerle, M. E.; Rebentrost, F.; Tributsch, H. *Electrochim. Acta* **1968**, *13*, 150. (d) Tributsch, H.; Gerischer, H. *Ber. Bunsen-Ges. Phys. Chem.* **1969**, *73*, 251. (e) Gerischer, H.; Willig, F. *Top Curr. Chem.* **1976**, *61*, 31. (f) Spitler, M.; Calvin, M. *J. Chem. Phys.* **1977**, *67*, 5193. (g) Memming, R. *Philips Techn. Rev.* **1978**, *38*, 160. (h) Fan, F. R. F.; Bard, A. J. *J. Am. Chem. Soc.* **1979**, *101*, 6139. (i) Takizawa, T.; Watanabe, T.; Honda, K. *J. Phys. Chem.* **1980**, *84*, 51. (j) Iwasaki, T.; Oda, S.; Sawada, T.; Honda, K. *Photogr. Sci. Eng.* **1981**, *25*, 6. (k) Borgarello, E.; Kiwi, J.; Pelizzetti, E.; Visca, M.; Grätzel, M. *Nature (London)* **1981**, *284*, 158. (l) Grätzel, M. *Acc. Chem. Res.* **1981**, *14*, 376. (m) Jaeger, C. D.; Fan, F. R. F.; Bard, A. J. *J. Am. Chem. Soc.* **1980**, *102*, 2592. (n) Watanabe, T.; Fujishima, A.; Honda, K. In *Energy Resources through Photochemistry and Catalysis*; Grätzel, M., Ed.; Academic Press: New York, 1983. (o) Hashimoto, K.; Kawai, T.; Sakata, T. *Nouv. J. Chim.* **1983**, *7*, 249. (p) Houlding, V. H.; Grätzel, M. *J. Am. Chem. Soc.* **1983**, *105*, 5695. (q) Shimidzu, T.; Iyoda, T.; Koide, Y.; Kanda, N. *Nouv. J. Chim.* **1983**, *78* 21. (r) Memming, R. *Prog. Surf. Sci.* **1984**, *17*, 7. (s) Riefkohl, J.; Rodriquez, L.; Romero, L.; Sampoll, G.; Souto, F. A. *J. Phys. Chem.* **1986**, *90*, 6068. (t) Hashimoto, T.; Sakata, T. *J. Phys. Chem.* **1986**, *90*, 4474.

(3) (a) Gerischer, H. *Ber. Bunsen-Ges. Phys. Chem.* **1973**, *77*, 771. (b) Gerischer, H. In *Photoelectrochemistry, Photocatalysis and Photoreactors*; Schiavello, M., Ed.; Reidel: Dordrecht, 1985; NATO ASI Series C, Vol. 148.

(4) (a) Matsumura, M.; Nomura, Y.; Tsubomura, H. *Bull. Chem. Soc. Jpn.* **1977**, *50*, 2533. (b) Matsumura, M.; Matsudaira, S.; Tsubomura, H.; Takata, M.; Yanagida, H. *I&E Prod. Res. Devel.* **1980**, *19*, 415.

(5) Alonso, N.; Beley, V. M.; Chartier, P.; Ern, V. *Rev. Phys. Appl.* **1981**, *16*, 5.

(6) Desilvestro, J.; Grätzel, M.; Kavan, L.; Moser, J.; Augustynski, J. *J. Am. Chem. Soc.* **1985**, *107*, 2988.

(7) Kalayanasundaram, K.; Vlachopoulos, N.; Krishnan, V.; Monnier, A.; Grätzel, M. *J. Phys. Chem.* **1987**, *91*, 2342. Vlachopoulos, N.; Liska, P.; McEvoy, A. J.; Grätzel, M. *Surf. Sci.* **1987**, *189*, 823.

(8) Vrachnou, E.; Vlachopoulos, N.; Grätzel, M. *J. Chem. Soc., Chem. Commun.* **1987**, 868.

(9) We formulate RuL_3 as a tetraanion. Acid–base titration shows the pH value for the first protonation to be 6.5. At pH <2.5 three more protons are added leading to the precipitation of the complex.

0002-7863/88/1510-1216$01.50/0

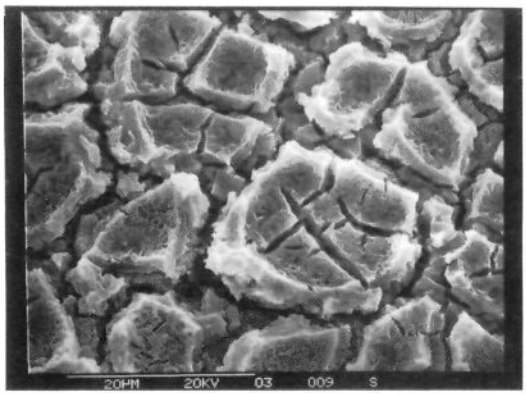

Figure 1. Scanning electron micrograph of the high surface area TiO_2 film used in the sensitization experiments.

with absolute methanol (Fluka puriss.) to give a titanium concentration of 25 or 50 mg/mL. The deposition of the oxide layer was carried out in a similar way as described by Stalder and Augustynski.[10] The tip of the TiO_2 rod was dipped in the titanium alkoxide solution containing 25 mg/mL of Ti. Excess solution was removed by tapping the electrode against the wall of the glass container. In the case of the 4 cm^2 Ti sheets, a droplet of the alkoxide solution was spread over the surface to produce a thin coating. Subsequently, the titanium alkoxide layer was hydrolyzed at room temperature for 30 min in a special chamber where the humidity was kept at 48 ± 1% of the equilibrium saturation pressure of water. The precise control of the humidity during the hydrolysis step turned out to be of crucial importance to obtain electrodes with high sensitization yields. The electrode was subsequently heated in air in a tubular oven kept at 450 °C. Preheating it in the entrance of the oven for 5 min was followed by 15 min of heating in the interior. Three more layers were produced in the same way. Subsequently, 10 thicker layers were deposited each by using the titanium alcoholate solution containing the higher Ti concentration, i.e., 50 mg/mL. The same procedure as for the first layers was applied except that the heating of the last layer lasted for 30 min. The total thickness of the oxide film was about 20 μ. The doping of the TiO_2 film was carried out by heating it in highly purified Ar (Air Liquide, Belgium, 99.997%). A horizontal tubular oven composed of quartz tubes with suitable joints was employed. After insertion of the electrodes, the tube was twice evacuated and purged with Ar. The electrode was then heated under Ar flux (2.5 L/h) at a rate of 500 °C/h up to 550 °C which was maintained for 35 min. The electrodes were removed after cooling.

A scanning electron micrograph of the TiO_2 layer produced in this way is shown in Figure 1. The high surface roughness is apparent from the presence of numerous pores and crevices in the film. The crystalline structure of the TiO_2 was examined by solid state Raman spectroscopy and was found to correspond to that of anatase.[11]

Dye Coating of the Electrode, Surface Roughness Factor, and Fractal-like Character of the TiO_2 Films. The RuL_3^{4-} was available from previous work.[6] It was coated onto the TiO_2 layer by dipping the electrode for 1 h in an aqueous solution (pH 3.5 adjusted with dilute HCl) containing 2×10^{-4} M RuL_3^{4-}. The TiO_2 film assumed an orange/red color due to adsorption of the dye. In acidic aqueous medium and in the absence of complexing agents such as EDTA[12] which compete for adsorption sites on the surface of TiO_2, the RuL_3^{4-} adhesion is irreversible, and no leaching of the dye into the solution could be detected at pH < 4 and moderately high electrolyte concentrations.

RuL_3^{4-} desorption from the TiO_2 surface occurs in alkaline medium and this was used to determine the surface roughness factor of the electrode. The RuL_3^{4-} coated TiO_2 sheet (geometric surface area 4 cm^2) was used in these experiments. Immersion in 10^{-2} M aqueous NaOH for 24 h resulted in complete desorption of the dye. The solution spectrum agreed with that for RuL_3^{4-}, and an extinction coefficient of 2.1×10^4 M^{-1} cm^{-1} at 470 nm was used in order to derive its concentration. This extinction coefficient was determined by recording the spectrum of a RuL_3^{4-} standard solution prepared by weighing out the dye. It is in agreement with an earlier literature value.[13] According to the results

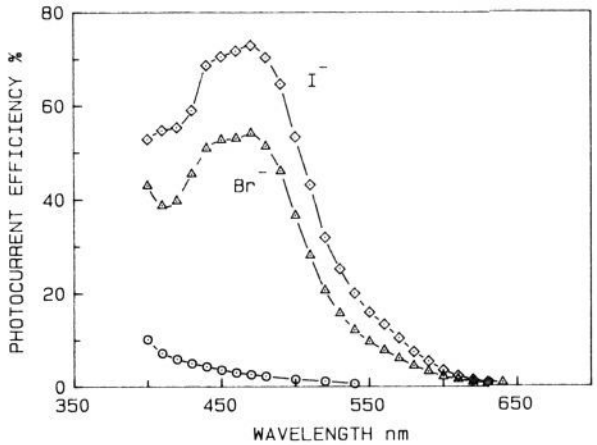

Figure 2. Photocurrent action spectrum for polycrystalline TiO_2 films in aqueous $HClO_4$ (10^{-3} M) containing LiBr or NaI as electron donor. The incident photon to current conversion efficiency (IPCE) is plotted as a function of excitation wavelength: (◇), RuL_3^{4-}-coated electrode 1 M KI; (△), RuL_3^{4-}-coated electrode 0.1 M NaBr; (○), bare TiO_2 film 10 μM hydroquinone.

of Furlong et al.,[12] one RuL_3^{4-} molecule occupies 100 $Å^2$ of TiO_2 surface at saturation monolayer coverage. On the basis of this area, the surface roughness factor is 181. This should be regarded only as a lower limit since the surface may contain micropores which are inaccessible to an adsorbent with the size of RuL_3^{4-}.[14]

We have performed preliminary studies aiming at characterizing the TiO_2 films in terms of a fractal-type dimension. It has been suggested that various porous materials have fractal structures or fractal pore structures over certain length scales.[15] A number of oxides have been analyzed as fractal structures.[16] In our investigation, we have employed impedance analysis of the TiO_2 films in contact with aqueous electrolyte following the method of Pajkossy.[17] The logarithm of the impedance was found to be a linear function of the logarithm of the frequency over several decades at constant phase angle. From the slope of the straight line the fractal dimension was estimated as 2.7. Although more detailed measurements are required to confirm the fractal nature and dimension of our TiO_2 electrodes, this result is instructive in as much as it confirms the spongelike character of the oxide film.

Methods. Photoelectrochemical experiments employed a three-compartment cell equipped with a quartz window, the auxiliary and reference electrode compartment being separated from the working electrode by glass frits. Potentials were adjusted with a Pine Instruments potentiostat. The regenerative photoelectrochemical cell consisted of the dye-loaded 2×2 cm TiO_2 sheet which was immersed in LiBr or NaI solution and a 3×3 cm sized Pt flag as counterelectrode. All solutions were thoroughly degassed with Ar.

An Oriel 450 W high pressure Xe lamp or a 250 W tungsten halogen lamp served as a light source and was employed in conjunction with a water filter and a Bausch & Lomb 300 nm blaze high intensity monochromater. The photon flux impinging on the cell was determined by a YSI Kettering Model 65A radiometer. In addition, chemical actinometry with ferrioxalate was performed. The actinometric solution consisting of 6 mL of 0.2 N $Fe_2(SO_4)_3$, 6 mL of 0.6 N potassium oxalate, and 68 mL of H_2O was directly placed in the photoelectrolysis cell and illuminated with the 420-nm output of the high pressure Xe lamp. The cell wall was covered with a black cloth equipped with a 2×2 cm sized light entrance window. This corresponds to the illuminated area of the TiO_2 sheet electrode in the photoelectrolysis experiments. The Fe(II) produced during the photolysis was analyzed colorimetrically as $Fe(bipy)_3^{2+}$ (ϵ(525 nm) 8240 M^{-1} cm^{-1} at pH 4.5). The light flux at 420 nm was determined to be $(5.0 \pm 0.25) \times 10^{-10}$ Einstein cm^{-2} s^{-1} as compared to 4.5×10^{-10} Einstein cm^{-2} s^{-1} derived from the thermoelectric measurements. The

(10) (a) Stalder, C.; Augustynski, J. *J. Electrochem. Soc.* **1979**, *126*, 2007. (b) Stalder, C. Ph.D. Thesis, Université de Genève.

(11) The Raman measurements were carried out by Prof. N. Error at the Oregon Graduate Center, OR, to whom we are grateful.

(12) Furlong, D. N.; Wells, D.; Sasse, W. H. F. *J. Phys. Chem.* **1986**, *90*, 1107.

(13) Foreman, C. Ph.D. Thesis, University of North Carolina, Chapel Hill, NC. We thank Prof. D. G. Whitten for providing us with a copy of this thesis.

(14) Avnir, D. *J. Am. Chem. Soc.* **1987**, *109*, 2931.

(15) (a) Even, U.; Rademann, K.; Jortner, J.; Manor, N.; Reisfeld, R. *Phys. Rev. Lett.* **1984**, *52*, 2164. (b) Avnir, D.; Farin, D.; Pfeifer, P. *Nature (London)* **1984**, *308*, 261.

(16) (a) Pfeifer, P.; Avnir, D.; Farin, D. *J. Stat. Phys.* **1984**, *36*, 699. (b) Schaefer, D. W.; Keefer, K. D. *Phys. Rev. Lett.* **1986**, *56*, 2199. (c) Rojanski, D.; Huppert, D.; Bale, H. D.; Dacai, X.; Schmidt, P. W.; Farin, D.; Seri-Levy, A.; Avnir, D. *Phys. Rev. Lett.* **1986**, *56*, 2505.

(17) Nyikos, L.; Pajkossy, T. *Electrochim. Acta* **1985**, *30*, 1533.

higher flux value obtained by chemical actinometry was used in the calculation of quantum yields.

Results and Discussion

Visible Light Induced Oxidation of Iodide and Bromide. Figure 2 shows the photocurrent action spectra for RuL_3^{4-}-coated TiO_2 films in 10^{-3} M $HClO_4$ in the presence of 1 M NaI and 0.1 M NaBr. For comparison, results obtained with the same electrode prior to dye coating are also presented. The incident monochromatic photon to current conversion efficiency (IPCE), defined as the number of electrons generated by light in the external circuit divided by the number of incident photons, is plotted as a function of the excitation wavelength. This was derived from the photocurrents by means of eq 1

$$\text{IPCE (\%)} = \frac{[(1.24 \times 10^3) \times \text{photocurrent density } (\mu A/cm^2)]}{[\text{wavelength (nm)} \times \text{photon flux } (W/m^2)]} \quad (1)$$

Although TiO_2 alone shows only a weak response in the visible, the RuL_3^{4-}-coated electrodes exhibited very high photocurrents. Thus, in the presence of 1 M KI, the photocurrent density at 470 nm at an incident light flux of 2.4 W/m was 66.4 $\mu A/cm^2$ which corresponds to an IPCE value of 73%. The achievement of such high conversion efficiencies in spectral sensitization is unprecedented. Matsumura et al.[4] have obtained an IPCE of 22% by using Al-doped sintered ZnO electrodes in conjunction with rose bengal as a sensitizer and iodide as a donor. Alonso et al.[5] achieved an IPCE of 1.5% with a similar electrode and alkyl-substituted $Ru(bipy)_3^{2+}$ as a sensitizer. The maximum IPCE we obtained previously[6] with RuL_3^{4-} in the presence of hydroquinone as electron donor was 44%. Upon repeating the experiment with 10^{-2} M hydroquinone and 0.1 M $LiClO_4/10^{-3}$ M $HClO_4$ electrolyte by using the same TiO_2 electrode as in Figure 4, an IPCE value of 74% was obtained at 460 nm. Thus, the maximum IPCE values for the iodide and hydroquinone are very similar. The increase in the IPCE with respect to our earlier result is attributed to the improved procedure in fabricating the TiO_2 films. In particular, the importance of controlling precisely the air moisture content during hydrolysis of the titanium alcoholate was not recognized during the earlier preparations. The present procedure gives significantly higher sensitization yields which are easily reproduced even on large area electrodes such as the 2 × 2 cm sized TiO_2 films.

The IPCE can be formulated as the product of the light harvesting efficiency and the quantum yield for charge injection

$$\text{IPCE} = (1 - I/I_o) \times \phi_{inj} = (1 - 10^{-\epsilon\Gamma})\phi_{inj} \quad (2)$$

where ϵ is the decadic extinction coefficient (units cm^2/mol) and Γ is the surface concentration (units mol/cm^2) of the dye. By using a roughness factor of 181 and an effective surface area of 100 $Å^2$ for RuL_3^{4-} and assuming that the extinction coefficient at 470 nm of the adsorbed RuL_3^{4-} is the same as that in aqueous solution, the light harvesting efficiency of a monolayer of RuL_3^{4-} at 470 nm is 78%. Since the IPCE value determined at this wavelength is 73%, a quantum yield for electron injection of 94% is derived. This is higher than the value of 60 ± 10% determined from laser photolysis experiments with colloidal TiO_2.[6] The difference could arise from structural factors. The interfacial morphology of the anatase film employed here may permit more intimate contact with the sensitizer than that present at the surface of the colloidal particles. The latter consist of a mixture of amorphous material and anatase. This increases the electronic coupling between the electronic wave function of excited RuL_3^{4-} and the 3d manifold of the TiO_2 conduction band resulting in a higher efficiency for charge injection. Multiple reflection of the light within the fractal-like structure of the TiO_2 layer could also contribute to the higher efficiency. (One referee pointed out that due to its very rough character, the electrode will scatter incident light extremely well. Consequently, the pathlength of the incident light is longer than a monolayer thickness, and the 78% figure for light harvesting may be too low. If 100% light harvesting efficiency is assumed at 470 nm, the quantum yield for electron injection is evaluated as 73% in better agreement with the result derived from the colloidal solutions.)

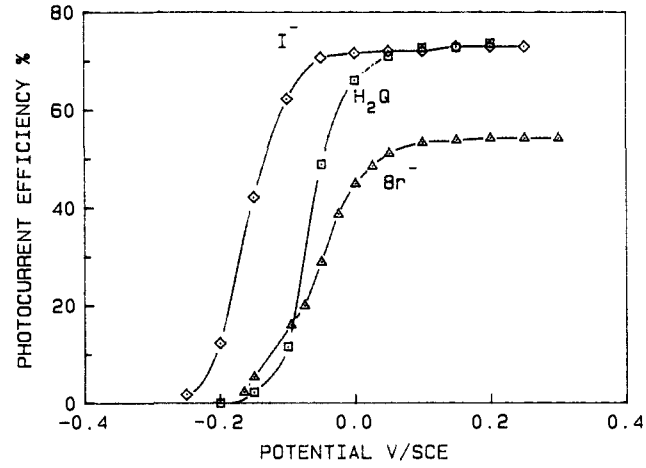

Figure 3. Photocurrent efficiency (IPCE)–potential curve recorded during 470-nm irradiation of a RuL_3^{4-}-coated TiO_2 film in aqueous 10^{-3} M $HClO_4$ containing (◇) 1 M KI; (□) 0.1 M hydroquinone + 0.1 M $LiClO_4$; (△) 0.1 M NaBr.

Figure 3 shows photocurrent–potential plots for solutions containing iodide, hydroquinone, or bromide as an electron donor. The photocurrent onset for the iodide-containing solutions is at −0.3 V (SEC), which is close to the flatband potential of the TiO_2 electrode which is −0.4 V at pH 3 in the absence of iodide. It is possible that the presence of I^- or I_3^- affects the value of V_{fb} as has been observed for GaAs.[18] Thereafter, the IPCE rises steeply, the plateau value of 73% being attained already at −0.1 V. The implication of this result is that relatively small band bending (~200 mV) within the depletion layer suffices to afford practically complete charge separation. This result is surprising in view of the polycrystalline nature of the TiO_2 layers. The defects and surface states present at the semiconductor solution interface are expected to act as recombination centers. That this is not the case is evident from the steep edge of the photocurrent–potential characteristic and rapid attainment of saturation. This indicates that recombination, i.e., recapture of conduction band electrons by the oxidized sensitizer (reaction 4) following charge injection,

$$*RuL_3^{4-} \xrightarrow{k_{inj}} RuL_3^{3-} + e_{cb}^-(TiO_2) \quad (3)$$

$$RuL_3^{3-} + e_{cb}^- \xrightarrow{k_b} RuL_3^{4-} \quad (4)$$

is slow even at small band bending within the TiO_2 film. These results contrast with the findings[19] obtained with ruthenium(II) bis(2,2′-bipyridyl)(2,2′-bipyridyldicarboxylate) chemically attached to TiO_2 where recapture of the photoinjected electrons was efficient even at large band bending resulting in a very poor quantum yield of sensitization, i.e., 0.25%. The current action spectrum observed with the attached latter dye is structureless indicating that the chemical derivatization of the TiO_2 surface produces semiconductor (t_{2g})/sensitizer surface states acting as recombination centers.[19] This sharply increases the rate of reaction 4 reducing drastically the efficiency of sensitization. The photocurrent action spectrum for RuL_3^{4-} matches its absorption characteristics indicating that this type of interaction is absent. Employing colloidal TiO_2 particles, the values of k_{inj} and k_b have been determined to be 3.2×10^7 and 4×10^5 s^{-1}, respectively.[6] Therefore, in the case of RuL_3^{4-}, the rate of electron injection in the TiO_2 conduction band is 80 times faster than that for recombination explaining the very effective light induced charge separation.

(18) van den Meerakker, J. E. A. M. *Electrochim. Acta* **1985**, *30*, 435.
(19) (a) Andersson, S.; Constable, E. C.; Dare-Edwards, M. P.; Goodenough, J. B.; Hamnet, A.; Seddon, K. R.; Wright, R. D. *Nature (London)* **1980**, *280*, 571. (b) Dare-Edwards, M. P.; Goodenough, J. B.; Hamnet, A.; Seddon, K. R.; Wright, R. D. *Faraday Discuss. Chem. Soc.* **1980**, *70*, 285. (c) Goodenough, J. P.; Hamnet, A.; Dare-Edwards, M. P.; Campet, G.; Wright, D. R. *Surf. Sci.* **1980**, *101*, 531.

The long term stability of the photocurrents in 0.1 M NaI solution was checked by exposing the RuL_3^{4-}-coated 4 cm^2 area TiO_2 film to polychromatic irradiation (Xe lamp, 420 nm cut-off filter). Upon illumination of the electrode with an incident light flux of 200 mW/cm^2, the photocurrent rose to 1.2 mA. It remained practically constant (fluctuations < 8%) during 100 h of illumination corresponding to 430 Coulombs of photoinduced charge and a turnover number of RuL_3^{4-} of 3.7×10^4.

The photocurrent onset observed with hydroquinone (HQ) as an electron donor is shifted by ca. 100 mV in the positive direction with respect to that of iodide, while for Br^- the displacement is ca. 150 mV. Apparently, the oxidation of these donors by RuL_3 at the TiO_2-solution interface (reactions 5 and 6 occurs at a smaller

$$2RuL_3^{3-} + HQ \rightarrow 2RuL_3^{4-} + 2H^+ + Q \quad (5)$$

$$2RuL_3^{3-} + 2Br^- \rightarrow 2RuL_3^{4-} + Br_2 \quad (6)$$

rate than that of iodide. At electrode potentials close to flat band condition, reactions 5 and 6 are not fast enough to compete with charge recombination. Therefore, no or very small photocurrents are observed. As the band bending increases, the rate constant for the back reaction 3 decreases resulting in a steep augmentation of the photocurrent. In the case of hydroquinone, the ICPE reaches a similar plateau value as for iodide. On the other hand, with bromide as a donor the maximum ICPE observed was lower, i.e., between 56 and 61%. This is likey to arise from partial bleaching of the dye in the photostationary state. If the incident light flux is high enough to render charge injection faster than reaction 6, a significant fraction of RuL_3^{4-} is converted to the oxidized form. This reduces the light energy harvesting efficiency of the device and hence its IPCE. A kinetic model of such processes has recently been published.[20]

The visible light induced oxidation of Br^- is an attractive reaction from the energy conversion point of view since Br_2 is a potent oxidant (E° = 0.85 V (SCE)). To our knowledge, the coupling of sensitization of large band gap semiconductors to the generation of bromine from bromide has so far not been achieved. The high redox potential of the RuL_3^{4-} sensitizer (E° = 1.32 V (SCE) for the protonated form[21]) is exploited here to drive this thermodynamically demanding process. In order to ascertain quantitatively the formation of bromine, a long term photolysis experiment was carried out. The TiO_2-covered Ti rod (geometric surface area 0.28 cm^2) was coated with RuL_3^{4-} and placed in 15.6 mL of solution containing 1 M LiBr and 10^{-3} M $HClO_4$. The $\lambda > 455$ nm output of the Xe lamp was focussed onto the electrode producing a photocurrent density of 2 mA/cm^2. The photoelectrolysis was interrupted after a charge of 25.3 C had passed corresponding to 3×10^4 turnovers of RuL_3^{4-}. The expected concentration of Br_2 in the solution is 8.1×10^{-3} M. The Br_2 was analyzed by reaction with I^- resulting in the formation of I_3^-,[22] and its concentration was determined as 5.8×10^{-3} M. This corresponds to 70% faradaic yield. The fact that the yield is smaller than 100% is attributed to consecutive reactions of Br_2, such as dismutation to hypobromide (equilibrium constant 10^{-4} at pH 3) and photoreduction of Br_2 by water to yield Br^- and oxygen.[23]

Regenerative Photoelectrochemical Cells Based on Dye Sensitization. The highly efficient sensitization of the TiO_2 films by RuL_3^{4-} can be exploited for the conversion of light into electric power by using a regenerative photoelectrochemical cell. A schematic illustration of such a device is shown in Figure 4. Light excitation of the sensitizer is followed by charge injection in the semiconductor producing the oxidized form of the dye and conduction band electrons. The original form of the sensitizer is reformed by reaction with an electron donor in the electrolyte. Regeneration of the reduced form of the donor occurs by reaction

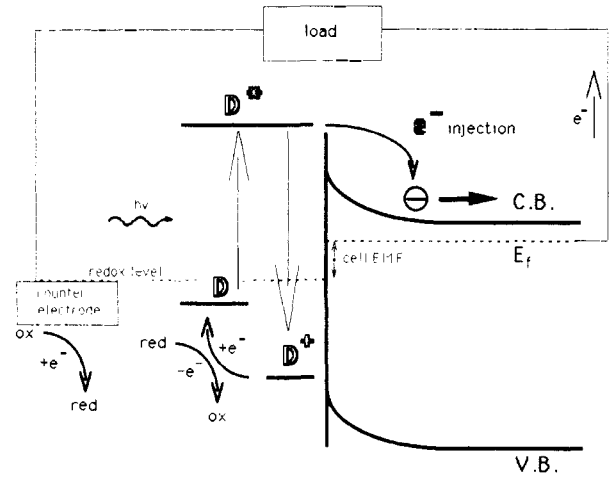

Figure 4. Schematic illustration of a regenerative photoelectrochemical cell based on dye sensitization.

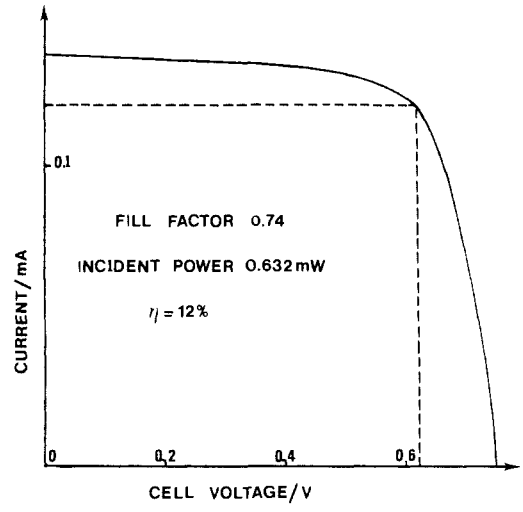

Figure 5. Photocurrent–voltage characteristics of a regenerative photoelectrochemical cell consisting of the RuL_3^{4-}-coated TiO_2 film (area = 4 cm^2) as photoanode and a Pt counterelectrode. Electrolyte contains 10^{-3} M $HClO_4$, 1 M LiBr, and 10^{-3} M Br_2. Excitation wavelength = 470 nm.

with the conduction band electrons at the cathode connected to the semiconductor through the external circuit. The electromotive force is given by the difference of the quasi-Fermi level of the conduction band electrons and the solution redox potential. For optimal conversion, the E° value of the donor should be as positive as possible. Therefore, the following studies were conducted with the Br_2/Br^- redox couple.

Figure 5 shows the current voltage characteristics of a cell consisting of the RuL_3^{4-}-coated 2 × 2 cm sized TiO_2 film as photoanode and a Pt counterelectrode. The aqueous solution contained 1 M LiBr, 10^{-3} M Br_2, and 10^{-3} M $HClO_4$. Monochromatic light of 470-nm wavelength and 1.58 W/m^2 intensity produced a short circuit current of 135 μÅ corresponding to an ICPE of 56.4%. As the load resistance or voltage is increased, the current at first stays fairly constant and then falls to zero at an open circuit voltage of 0.75 V. The maximum power delivered is represented by the area of the largest rectangle that can be fitted under the curve: in this case 0.75 mW at 0.62 V. A measure of squareness of the characteristic is the fill factor defined as

$$\text{fill factor} = \text{maximum output power}/(\text{short circuit current} \times \text{open circuit voltage})$$

From Figure 5 the fill factor is determined as 0.74 which is astonishingly high for a device based on a polycrystalline semi-

(20) Desilvestra, J.; Duonghong, D.; Kleijn, M.; Grätzel, M. *Chimia* **1985**, *39*, 102.
(21) Spitler, M. T. *J. Electroanal. Chem.* **1987**, *228*, 69.
(22) Kiwi, J.; Grätzel, M. *Chem. Phys. Lett.* **1981**, *78*, 241.
(23) Remy, H. *Treatise on Inorganic Chemistry*; Elsevier: Amsterdam, Houston, London, New York, 1956; Vol. 1, p 784.

conductor film. This indicates that the loss mechanism, such as recombination, normally encountered in semiconductor photoelectrochemistry, has been minimized. The performance characteristics achieved here are comparable to those of high quality single crystal photovoltaic cells. The conversion efficiency is the maximum power output expressed as a percentage of the input light power

$$\eta(\%) = \text{maximum output power} \times 100/(\text{irradiance} \times \text{area})$$

Figure 5 gives $\eta = 12\%$ for 470-nm light which is by far the highest monochromatic conversion yield achieved until now in dye sensitized regenerative photoelectrochemical cells. The maximum monochromatic efficiency reported previously by Matsumara et al.[4] is 2.5% for 540-nm light and sintered ZnO pellets coated with rose bengal as a sensitizer.

We finally report preliminary findings obtained with the RuL_3^{4-}-sensitized regenerative cell by using polychromatic light excitation. The conditions used were the same as in Figure 5 except that the concentration of LiBr was 0.1 M and that the entire $\lambda > 420$ nm light output of the high pressure Xe lamp was used for excitation of the RuL^{4-}-coated 2×2 cm sized TiO_2 film. The light power incident on the 4 cm^2 TiO_2 sheet was 174 mW. Open circuit voltage was 0.92 V, and the short circuit current was 3.4 mÅ. Maximum power output was 2.1 mW at a cell voltage of around 0.73 V corresponding to a fill factor of 0.67 and a conversion efficiency of 1.2%. Decreasing the incident power by a factor of 10 resulted in an increase of η to 1.6%. These performance parameters may be further improved by optimizing the experimental conditions. Also, it should be noted that polychromatic efficiencies depend on the emission features of the light source. Sunlight experiments will provide the solar conversion characteristics.

Conclusions

The findings presented here confirm the very promising properties of high surface area anatase films employed in conjunction with suitable sensitizers, as visible light energy harvesting and conversion devices. RuL_3^{4-}-coated films display incident monochromatic photon to current conversion efficiencies of up to 74%. Turnover numbers exceeding several 10 000 show the extremely rugged character of this chromophore, the quantum yield for destructive side reactions being below 10^{-5}. Another attractive feature of RuL_3^{4-} is the high redox potential in the ground state allowing the sensitized electron injection in the semiconductor to be coupled to thermodynamically demanding oxidation reactions. The present report focusses on the oxidation of halide ion. For the first time the sensitized generation of Br_2 from Br^- is achieved at a large band gap semiconductor electrode. This reaction is exploited to generate electrical power in a photodriven electrochemical cell. Even without optimization, a monochromatic conversion efficiency as high as 12% and a fill factor of 0.74 have been obtained. Due to their durability, low cost, and high efficiency these systems appear to have the potential to serve in practical solar energy conversion devices.

Acknowledgment. This work was supported by the Gas Research Institute, Chicago, IL (subcontract with the Solar Energy Research Institute (SERI), Golden, CO), the Swiss National Energy Foundation (NEFF), and the Swiss Office for Energy (OFEN). We are grateful to Dr. Ersi Vrachnou for assistance with the chemical actinometry. We also acknowledge discussions with Prof. Martin Fleischmann, University of Southampton, U.K., concerning the fractal character of the TiO_2 film.

Registry No. RuL_3^{4-}, 78338-26-8; TiO_2, 13463-67-7; Br_2, 7726-95-6; LiBr, 7550-35-8; KI, 7681-11-0; NaBr, 7647-15-6; $HClO_4$, 7601-90-3; hydroquinone, 123-31-9.

Structural Effect of *gem*-6 Substitution on C, N, P, S, and O Atoms: Crystallographic Data Analysis of Numerous C_3CZCC_3 Fragments. Modelization of Static and Dynamic Molecular States

Jacques-Emile Dubois* and Aliette Cossé-Barbi

Contribution from the Institut de Topologie et de Dynamique des Systèmes de l'Université Paris 7, Associé au CNRS, 1, Rue Guy de la Brosse, 75005 Paris, France. *Received July 10, 1985. Revised Manuscript Received September 19, 1987*

Abstract: C_3CZCC_3 fragments show systematic distortions of local symmetries when compared with structures chosen as formal references. Interactions between groups lead the structure to search for stable shapes by complex processes involving both *rotational* and *framework distortions*. In acyclic series tertiary groups avoid each other by a conrotatory rotational process (static gear effect), while in cyclic series (six-membered ring) the process is disrotatory and the twist conformers are forbidden. In the conformational ϕ_1, ϕ_2 mean torsion angle space, this leads to an *impressive sectorization of acyclic fragments in quadrants 1 and 3* ($\phi_1 \times \phi_2 > 0$) *and cyclic ones in quadrants 2 and 4* ($\phi_1 \times \phi_2 < 0$). Framework distortions (FRAM.DST.) are distributed throughout the entire fragment. They involve a significant opening of angle CZC (CZC BEND.), the symmetrical deformation of C_3C groups by contraction or expansion, and the C_3C tilt. Thus, four basic strain release effects (ROT.DST., CZC BEND., CC_3 SYM.DEF., CC_3 TILT) exist in all the subclasses examined (Z = C_{sp^3}, C_{sp^2}, NO, NH, NMe, P, cyclic, or acyclic fragments) with different amplitudes. They are *interdependent* among themselves and are a function of the hybridization of the Z atom. In each subpopulation, their mean value provides a basis for *predicting* new strain geometries. Correlated rotations and CZC bending are equally efficient in reabsorbing steric energy (MM simulation in a model compound). Any one of these two effects without the other accounts for some two-thirds of the steric strain release at the most. Despite crowding, the conformational flexibility of C_3CZCC_3 fragments remains considerable. Their shape variations are dynamically associated with some framework deformation steps all along the interconversion pathways. Thus, the smaller apparent size of tertiary groups results from the *cooperative interaction* of framework distortions and specific rotational processes, the former lowering the energy barriers (from several hundred to several kilocalories/mole; INDO and MM calculations) of the interconversion pathways forbidden with standardized molecular frameworks.

Crowded systems, in particular those with two tertiary groups in *gem* position, have certain specificities that have been approached in two different ways: studying property variations in families by progressive substitution and comparing C_3CZCC_3

0002-7863/88/1510-1220$01.50/0